

## Original article

## CoMFA analysis of dual/multiple PPAR activators

Palak Shah <sup>a</sup>, Amit Mittal <sup>b</sup>, Prasad V. Bharatam <sup>a,\*</sup><sup>a</sup> Department of Medicinal Chemistry, National Institute of Pharmaceutical Education and Research, Sector 67, S.A.S. Nagar, Punjab 160062, India<sup>b</sup> Department of Pharmaceutical Technology, National Institute of Pharmaceutical Education and Research, Sector 67, S.A.S. Nagar, Punjab 160062, India

Received 21 July 2007; received in revised form 30 December 2007; accepted 10 January 2008

Available online 30 January 2008

## Abstract

Dual or multiple activators are agents which act at more than one biological target and produce synergistic therapeutic effect. Computational methods can be successfully employed in designing dual activators. 'Additivity of molecular fields' concept was recently introduced to help design new dual activators. This concept is employed in this work to explore the scope and limitations of the concept, with the help of reported PPAR $\alpha/\gamma/\delta$  multiple activators. Three individual CoMFA models were first generated, followed by dual and multiple models. Dual PPAR $\alpha/\gamma$  CoMFA model could be developed successfully. However, dual PPAR $\gamma/\delta$ , dual PPAR $\alpha/\delta$  and multiple PPAR $\alpha/\gamma/\delta$  CoMFA models could not be very well developed. This follows from the poor correlation observed in the PPAR $\delta$  CoMFA model.

© 2008 Elsevier Masson SAS. All rights reserved.

**Keywords:** CoMFA; Anti-diabetic; PPAR; Additivity of molecular fields; 3D QSAR; Dual activators

## 1. Introduction

Designing dual/multiple activating drugs is an emerging drug design paradigm [1]. Dual/multiple activators act at more than one biological target selectively and produce synergistic therapeutic influence. Morphy and Rankoic preferred to label them as Designed Multiple ligands (DML) to highlight the rational design approach which is in practice and the multiple biological profile of these systems. Most often their biological targets belong to the same receptor super family. Dual/multiple activators differ from non-selective ligands in a way that the latter act on a gamut of receptors, leading to side effects. Dual and multiple activators exhibit simpler pharmacokinetic and pharmacodynamic profiles as compared to multicomponent drug therapy. Multiple activator design strategies can be generally classified into two major categories pharmacophore combination approach and screening approach [2]. Out of all the dual activators identified until now, most of them are dual antagonists or dual inhibitors. A few selected examples are given below: (Fig. 1) (i) Dual

inhibitors of Thymidylate Synthase (TS) and Dihydrofolate Reductase (DHFR) evaluated by National Cancer Institute [3,4] (A), (ii) multiple acting ligands such as COX-1, COX-2 and 5-LOX inhibitors e.g. Tepoxaline, designed using pharmacophore combination approach (B) [5–7] and (iii) Dual cardioselective calcium channel agonist and a smooth muscle selective calcium channel antagonist indicated in the treatment of congestive heart failure (C) [8].

Computational methodologies are quite suitable for the design of dual activators. Molecular docking, pharmacophore mapping, *de novo* design and QSAR methods can be successfully employed to gain an insight into dual activation and in the design of dual activators. One such example was recently reported from our lab, exploiting 'additivity of molecular fields' concept in the backdrop of CoMFA [9]. Selectivity and additivity of molecular fields are relatively new concepts introduced in molecular field analysis. Zefirov and co-workers addressed the problem of pairwise selectivity by using the difference between biological activities expressed as  $-\log K_i$  at receptor subtypes as dependant variable to develop CoMFA model [10]. The resulting selectivity fields indicated ways to increase the binding selectivity at either receptors. We addressed the question of dual activity in a similar way, using

\* Corresponding author. Tel.: +91 172 2214684.

E-mail address: [pvbharatam@niper.ac.in](mailto:pvbharatam@niper.ac.in) (P.V. Bharatam).

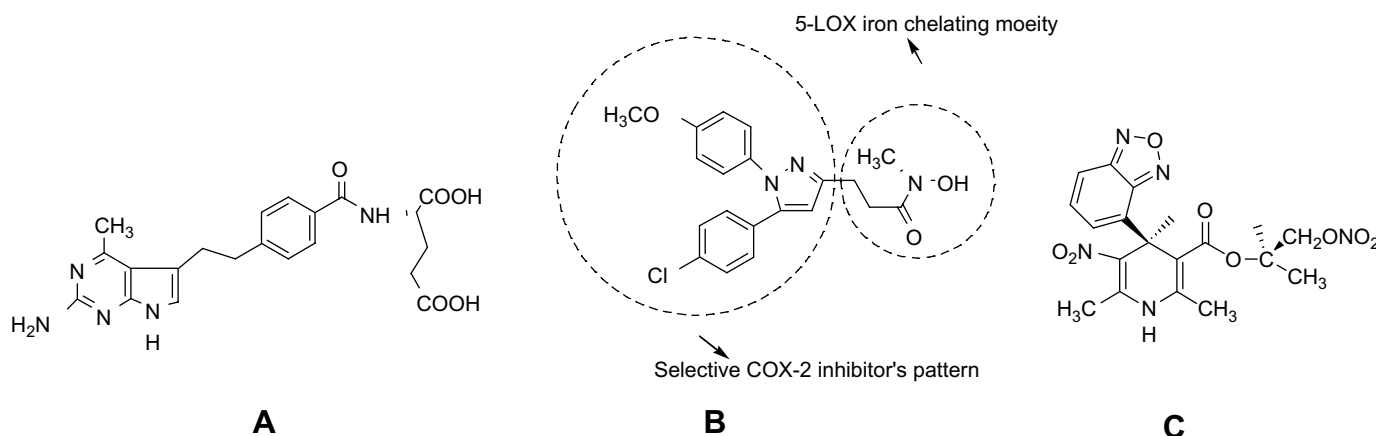


Fig. 1. Dual inhibitors.

sum of biological activities ( $pIC_{50}$ ), as dependant variable to develop a dual CoMFA model and reported that dual CoMFA models showed better statistical significance than the individual CoMFA models. It was also shown that a comparative approach in analysis of dual and individual CoMFA models proved to be useful in designing novel dual activators. The newly designed dual activators were validated with the help of molecular docking analysis. A possible limitation of the additivity concept is that for a dual CoMFA model to be successful, it should be built from a series of compounds which show similar potencies. A few questions still need to be addressed in this regard: (a) whether this concept has universal acceptability or not, (b) whether this concept is extendable to multiple activator design or not, (c) what are the scope and limitations of this concept. To verify these questions we have taken up CoMFA study.

Insulin resistance, dyslipidemia and obesity can be seen as components of a complex mixture of abnormalities known as 'metabolic syndrome' or syndrome X. This has stimulated interest in developing dual and multiple PPAR agonists. (Various dual/multiple activators for PPAR $\alpha/\gamma$ , PPAR $\alpha/\gamma/\delta$  agonists are in phase III clinical trials.) PPAR $\alpha$  plays a pivotal role in the uptake and oxidation of fatty acids and also in lipoprotein metabolism [11,12]. PPAR $\alpha$  agonists which play a significant role in lowering circulating lipids are used in hyperlipidemia. PPAR $\gamma$  which is predominantly expressed in adipose tissue is a key modulator of adipocyte differentiation [13]. PPAR $\gamma$  activators exemplify anti-diabetic effects via increasing insulin sensitivity of adipose tissue and skeletal muscle. Several studies have been carried out on PPAR $\gamma$  in our lab, both independently and in collaboration with the industry [14–20]. PPAR $\delta$  has been recognized as one of the targets in Syndrome X. PPAR $\delta$  agonists may provide a new approach to the treatment of cardiovascular disease by promoting reverse cholesterol transport [21]. The benefit of targeting PPAR $\delta$  is that it is ubiquitously expressed in many tissues, unlike PPAR $\alpha$  and PPAR $\gamma$ , which are expressed in a tissue specific manner. A drug with PPAR $\alpha/\gamma/\delta$  triple activating ability seems to improve the insufficiencies of the current therapeutic intervention of Type 2 diabetes. Recently, a series of  $\alpha$ -isopropoxy-phenylpropanoic

acids containing oxadiazole tails was reported [22] to be potent and efficacious against all three human PPAR subtypes (hPPAR $\alpha$ , hPPAR $\gamma$  and hPPAR $\delta$ ). Though this series of compounds are only partial agonists, they may be subjected to correlation analysis between structure and activity. The above mentioned series was used in the development of individual/dual and multiple CoMFA models to explore the stretchability of additivity concept.

## 2. Materials and methods

### 2.1. Data sets

A data set of 23 compounds of a series of oxadiazole-substituted  $\alpha$ -isopropoxy phenylpropanoic acids [22] (Table 1) was chosen to develop the following CoMFA models:

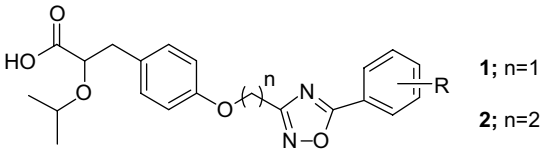
- Individual  $\alpha$ ,  $\gamma$ ,  $\delta$  CoMFA models
- Dual  $\alpha/\gamma$ ,  $\gamma/\delta$ , and  $\alpha/\delta$  CoMFA models
- Multiple  $\alpha/\gamma/\delta$  CoMFA model

The biological activities reported as  $EC_{50}$  values were converted to  $pEC_{50}$  in nanomolar/molar terms and were used as dependant variables in CoMFA. In the development of dual/multiple CoMFA models,  $pEC_{50}$  values were defined as sum of individual  $pEC_{50}$  values.

### 2.2. Minimization and alignment

Ligands under study were built employing the SKETCH module of SYBYL 6.9 [23] molecular modeling package installed on a Silicon Graphics workstation with IRIX 6.5 operating system. Crystal structures of PPAR $\gamma$  complexed with GW 409544 (PDB code: 1K74 [24]) PPAR $\alpha$  complexed with GW 409544 (PDB code: 1K7L [24]) and PPAR $\delta$  complexed with GW 2433 (PDB code: 1GWX [25]) are known. The basic skeleton and conformation of the most active molecule **1n** (having good activity at all three receptors) was modeled using AM1 minimized extracted ligands from 1K7L. AM1, a semi-empirical method of minimization in MOPAC module of

Table 1  
Transient transfection data of PPAR agonists **1** and **2** used for CoMFA models<sup>a</sup>



Compounds	R	EC <sub>50</sub> <sup>b</sup> (nM)	EC <sub>50</sub> <sup>b</sup> (nM)	EC <sub>50</sub> <sup>b</sup> (nM)
		hPPAR $\alpha$	hPPAR $\gamma$	hPPAR $\delta$
<b>1a</b>	H	160	79	10,000
<b>1b</b>	3-F	79	100	7900 <sup>c</sup>
<b>1c</b>	4-F	160	200	7900 <sup>c</sup>
<b>1d</b>	2-Me	40	100	1600 <sup>c</sup>
<b>1e</b>	3-Me	79	50	1600 <sup>c</sup>
<b>1f</b>	4-Me	25	16	2500 <sup>c</sup>
<b>1g</b>	4-Cl	13	20	500 <sup>c</sup>
<b>1h</b>	4-Br	40	32	790 <sup>c</sup>
<b>1i</b>	4-CF <sub>3</sub>	32	25	500 <sup>c</sup>
<b>1j</b>	4-CF <sub>3</sub> O	20	63	7900 <sup>c</sup>
<b>1k</b>	4- <i>i</i> -Pr	13	4	7900 <sup>c</sup>
<b>1l</b>	4- <i>t</i> -Bu	40	3	5000 <sup>c</sup>
<b>1m</b>	3,5-Di-F	40	100	160 <sup>c</sup>
<b>1n</b>	3,5-Di-CF <sub>3</sub>	6	32	320 <sup>c</sup>
<b>1o</b>	Cyclohexyl <sup>c</sup>	240	230	— <sup>d</sup>
<b>2a</b>	H	2000	13	— <sup>d</sup>
<b>2b</b>	3-F	500	2	4000 <sup>c</sup>
<b>2c</b>	4-F	790	40	— <sup>d</sup>
<b>2d</b>	4-Cl	400	25	— <sup>c</sup>
<b>2e</b>	3-Cl	320	4	100 <sup>c</sup>
<b>2f</b>	3-CF <sub>3</sub>	200	6	500 <sup>c</sup>
<b>2g</b>	2-CF <sub>3</sub>	400	160	2500
<b>2h</b>	3,5-Di-CF <sub>3</sub>	50	4	— <sup>d</sup>
<b>2i</b>	3- <i>t</i> -Bu, 5-CF <sub>3</sub>	— <sup>f</sup>	— <sup>f</sup>	— <sup>f</sup>

<sup>a</sup> Molecules used in test set includes (**1a**, **1d**, **1e**, **2a** for PPAR $\alpha$ ), (**2b**, **2c**, **2d**, **2g** for PPAR $\gamma$ ), (**1a**, **1b**, **1f**, **1g**, **2e** for PPAR $\delta$ ), (**1g**, **1o**, **2b**, **2e** for PPAR $\alpha/\gamma$ ), (**1b**, **1g**, **1k**, **1m** for PPAR $\gamma/\delta$ ), (**1c**, **1j**, **2e**, **2f** for PPAR $\alpha/\delta$ ), (**1f**, **1m**, **2e**, **2g** for PPAR $\alpha/\gamma/\delta$ ).

<sup>b</sup> Compounds were assayed for agonistic activity on PPAR-GAL4 chimeric receptors in transiently transfected CV-1 cells as described; EC<sub>50</sub> = the concentration of test compound that gave 50% of maximal reporter activity.

<sup>c</sup> Compound with percent activation 40–70%.

<sup>d</sup> Compounds with percent activation <40%.

<sup>e</sup> Cyclohexyl directly attached to oxadiazole. All data  $\pm 15\%$  ( $n = 3$ ).

<sup>f</sup> Newly designed molecule.

SYBYL 6.9, maintains the ‘U’ shape essential for activity [26]. AM1 minimized **1n** served as a template for building rest of the molecules which were cleaned up and minimized in a similar manner. All compounds in this series are chiral; *S*-enantiomers have been chosen for this study as they are reported to be more active than the *R*-enantiomers. Partial atomic charges estimated using Mulliken method were assigned to all atoms in the chosen molecules [27]. The ‘alignment rule’ which describes the positioning of a molecular model within the fixed lattice is very important input variable in CoMFA, since the relative interaction energies depend strongly on relative molecular positions [28]. It is preferable to choose an alignment which maintains the bioactive conformation (U shape as in rosiglitazone). The present work includes a combination of fit-atom and FlexS methods for alignment (Fig. 2).

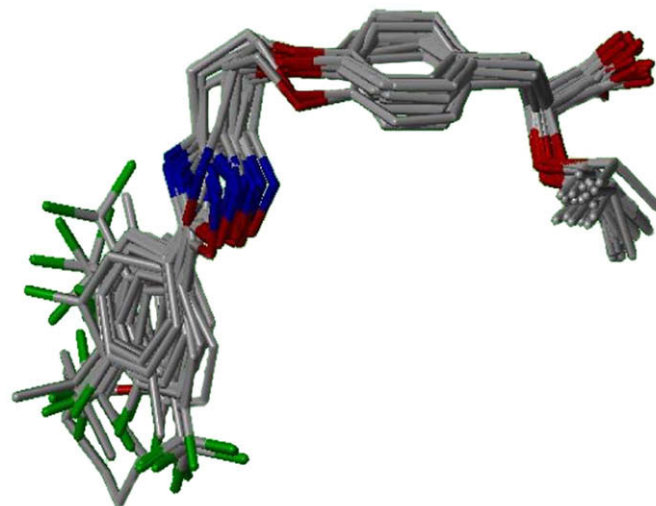


Fig. 2. Alignment of the compounds of the data set for PPAR $\alpha$  receptor.

### 2.3. CoMFA 3D QSAR models

The standard TRIPOS settings were used to carry out CoMFA analysis. CoMFA fields were derived by automatic calculations of energies of steric and electrostatic interactions between the compounds of interest and a probe atom. The probe atom was placed at various intersections of a regular 3D lattice, large enough to surround all compounds in the series, and with a 2 Å separation between the lattice point unless otherwise stated. An sp<sup>3</sup> carbon atom was used as a probe atom to generate steric field energies (Lennard–Jones potential) and charge of +1 to generate electrostatic field energies (coulombic potential). A distance dependant dielectric constant of 1.00 was used. Steric and electrostatic fields were truncated at +30.00 kcal/mol.

### 2.4. Partial Least Squares (PLS)

This statistical method was used to linearly correlate the CoMFA fields to the binding affinity values. The cross-validation analysis was performed using Leave-One-Out (LOO) method. The cross-validated  $r^2(r_{cv}^2)$  that resulted in optimum number of components and lowest standard error of prediction were taken. Equal weights were assigned to steric and electrostatic fields using CoMFA\_STD scaling option. To speed up the analysis and to reduce noise, a minimum filter value  $\sigma$  of 2.00 kcal/mol was used. Final analysis was performed to calculate conventional  $r^2(r_{ncv}^2)$  using the optimum number of components obtained from the cross-validation analysis.

## 3. Results and discussion

### 3.1. Statistical analysis of individual CoMFA models

Three independent CoMFA models were built: (i)  $\alpha$  model, based on  $pEC_{50}$  values for PPAR $\alpha$  as the dependant variable, (ii)  $\gamma$  model, based on  $pEC_{50}$  values of the ligands to PPAR $\gamma$

Table 2  
CoMFA Statistics of  $\alpha$  model,  $\gamma$  model and  $\delta$  model

Parameters	$\alpha$ model	$\gamma$ model	$\delta$ model
$n$	19	19	13
$n_1$	4	4	5
$r_{cv}^2$	0.687	0.633	0.509
ONC	4	5	5
$r_{ncv}^2$	0.988	0.999	0.995
SEE	0.078	0.017	0.052
$F$ values	287.006	4065.000	293.348
Steric	0.668	0.551	0.459
Electrostatic	0.332	0.449	0.541

$n$  = No. of molecules in training set;  $n_1$  = no. of molecules in test set; ONC = optimum number of components; steric = steric field contributions; electrostatic = electrostatic field contributions.

and (iii)  $\delta$  model, based on  $pEC_{50}$  values of ligands for PPAR $\delta$  receptor. Final CoMFA models were chosen after rigorous cycles of model development and validation based on internal predictions of the training set and the external predictions of the test set. The statistical parameters for the three models developed are shown in Table 2. Both  $\alpha$  and  $\gamma$  models show

better statistical results than  $\delta$  model.  $\alpha$  Model shows cross-validated  $r^2(r_{cv}^2)$  of 0.687 with four components and non-cross-validated  $r^2(r_{ncv}^2)$  of 0.988 while the corresponding values for the other two models are 0.633 with three components and 0.999 for  $\gamma$  model and 0.509 with five components and 0.995 for the  $\delta$  model. The statistical errors in this model are also reasonably low amounting to 0.078 for  $\alpha$  model, 0.017 for  $\gamma$  model and 0.052 for  $\delta$  model as indicated by the internal and external predictions of the training and test set molecules. The steric and electrostatic field contributions for the  $\alpha$  model are 0.688 and 0.332, respectively, for the  $\gamma$  model the values are 0.551 and 0.449, respectively, and for the  $\delta$  model, they are 0.459 and 0.541, respectively. The residuals calculated for all three individual models were found to be low in magnitude emphasizing good predictive ability of the developed CoMFA models (Fig. 3). The statistical data of the  $\delta$  model is poor and indicates that the reported PPAR $\delta$  data is poorly correlated. The residuals calculated for  $\alpha$  and  $\gamma$  models were lower as compared to those calculated for the  $\delta$  model. The  $\delta$  model was found statistically weak. This could be explained by the tight range of activity of the training set molecules.

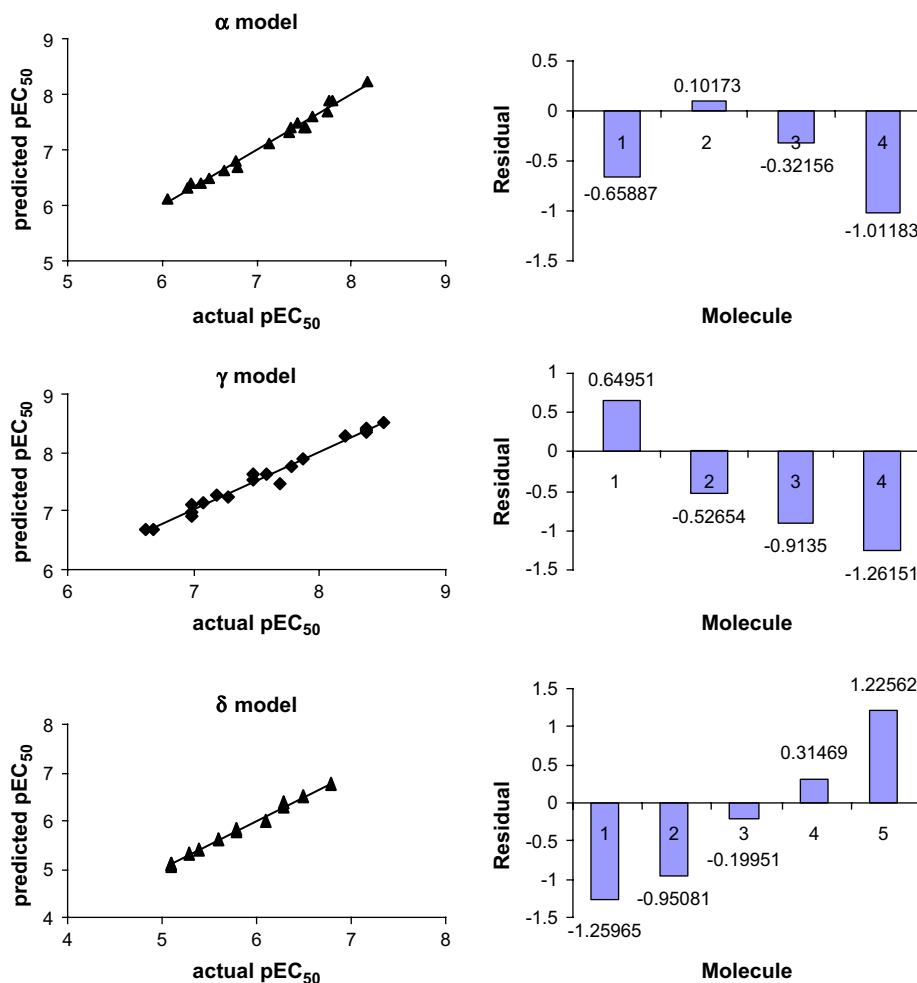


Fig. 3. Scatter plots showing actual vs. predicted  $pEC_{50}$  values of training set molecules and bar diagram showing residual values in test set of compounds of  $\alpha$  model,  $\gamma$  model,  $\delta$  model,  $\alpha/\gamma$  model,  $\gamma/\delta$  model,  $\alpha/\delta$  model,  $\alpha/\gamma/\delta$  model, respectively.

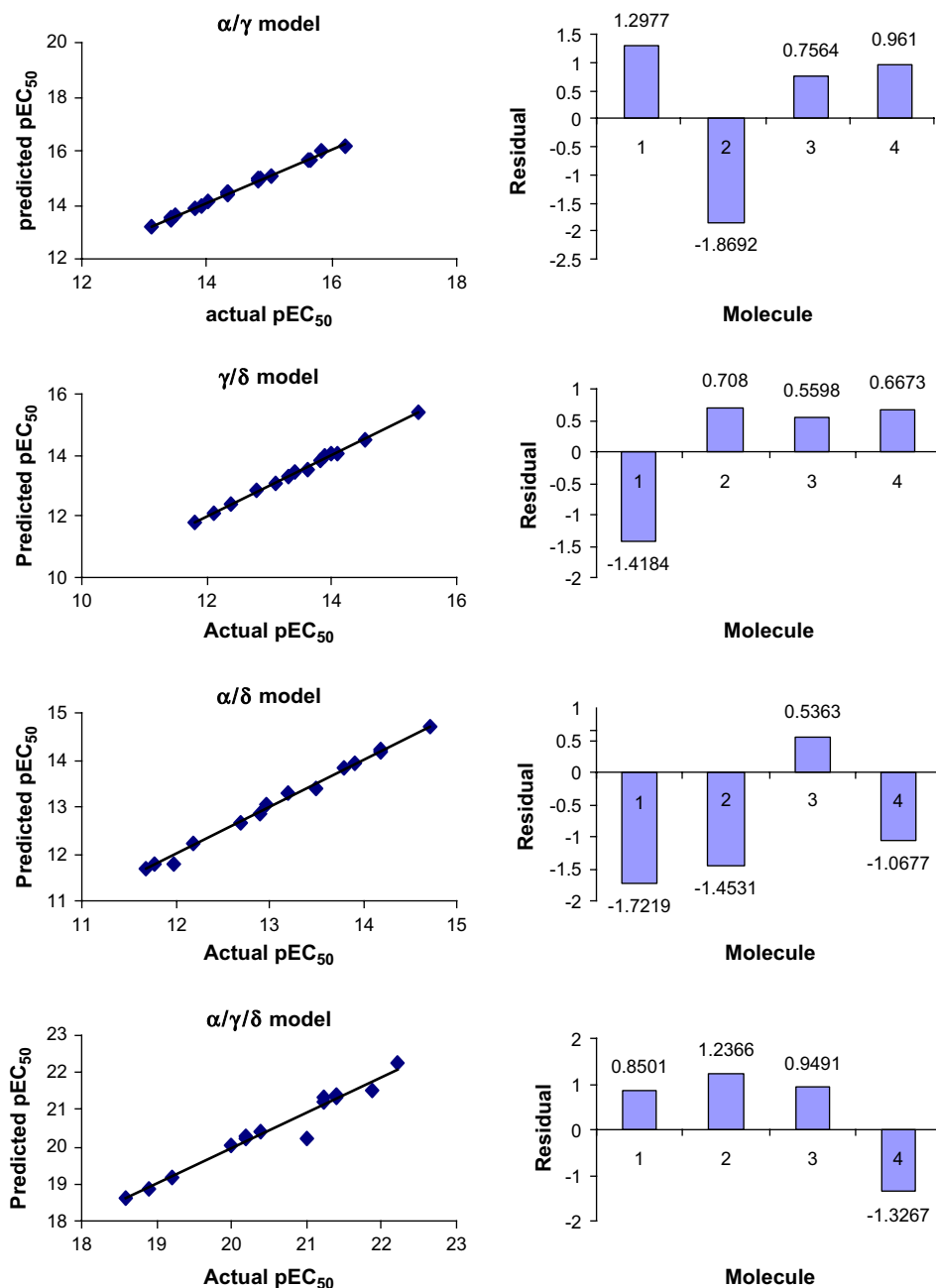


Fig. 3. (Continued).

Moreover, most of the studied molecules are not active against PPAR $\delta$ .

### 3.2. Statistical analysis of dual and multiple CoMFA models

Three dual models, dual  $\alpha/\gamma$ , dual  $\gamma/\delta$  and dual  $\alpha/\delta$ , were built on the addition of binding affinities of the ligands to PPAR $\alpha$ , PPAR $\gamma$  and PPAR $\delta$  receptors. These additive values of  $pEC_{50}$  represent the combined fields or the additivity fields for two receptors. Out of the three dual models, dual  $\alpha/\gamma$  model showed best statistical results with cross-validated

$r^2(r_{cv}^2)$  is 0.756 and non-cross-validated  $r^2(r_{ncv}^2)$  is 0.998 (Table 3). The statistical error in this model is reasonably low amounting to 0.049. The steric and electrostatic contributions are 0.691 and 0.309, respectively. This model, being statistically better, reveals more information than individual  $\alpha$  and  $\gamma$  CoMFA models.  $\alpha/\gamma$  Dual model is able to predict the combined biological activities for both PPAR $\alpha$  and PPAR $\gamma$  receptors. The above model is expected to identify molecules which act at both PPAR $\alpha$  and PPAR $\gamma$  receptors i.e. any molecule which shows activity in the dual model is able to show activity in both  $\alpha$  and  $\gamma$  models. As compared to individual CoMFA models and  $\alpha/\gamma$  dual model, the other



Table 3  
CoMFA statistics of dual and multiple models

Parameters	$\alpha/\gamma$	$\gamma/\delta$	$\alpha/\delta$	$\alpha/\gamma/\delta$
$n$	19	13	14	14
$n_1$	4	5	4	4
$r_{cv}^2$	0.756	0.233	0.267	0.430
ONC	5	5	5	3
$r_{ncv}^2$	0.998	0.999	0.998	0.988
Standard error of estimate	0.049	0.050	0.052	0.163
$F$ values	1248.418	1083.382	910.447	197.994
Steric	0.691	0.607	0.540	0.557
Electrostatic	0.309	0.393	0.460	0.443

$n$  = No. of molecules in training set;  $n_1$  = no. of molecules in test set; ONC = optimum number of components; steric = steric field contributions; electrostatic = electrostatic field contributions.

two dual models and multiple models showed poor statistical results. The cross-validated  $r^2(r_{cv}^2)$  and non-cross-validated  $r^2(r_{ncv}^2)$  for  $\gamma/\delta$  model are 0.233 and 0.999, respectively, with five components while the corresponding values for  $\alpha/\delta$  dual model are 0.267 and 0.998, respectively, with five components. For the multiple model, the corresponding values are 0.430 and 0.988, respectively, with three components. Though the SEE values are relatively small, these models are not reliable. All attempts to realize better correlation for these models failed. On the basis of these results it can be concluded that only the PPAR $\alpha$  and PPAR $\gamma$  data are statistically co-relatable, using additivity concept. When PPAR $\delta$  data was employed, “additivity concept” did not lead to reliable correlation. This may be attributed mainly to the poor correlation that existed within PPAR $\delta$  data and to the large difference in the EC<sub>50</sub> values of PPAR $\delta$  with respect to that of PPAR $\alpha$  and PPAR $\gamma$ .

### 3.3. Contour analysis

CoMFA is a model of the relationship between molecular field differences of a set of molecules and differences in their biological activity. Molecular fields are defined in terms of the interaction energies of some probe atoms placed at the nodes of a grid surrounding the molecules. A ‘field fit’ of the molecular fields with known biological activities leads to colored contour maps, after Partial Least Squares (PLS) analysis, which indicates the required field changes while designing new molecules. The steric contour maps are represented in green and yellow while the electrostatic contour maps are represented in red and blue. The green contours are indicative of regions favorable for sterically bulky substituents and the yellow contours are indicative of regions that are sterically less favorable. In a similar way the red contours represent regions that lead to the enhancement of activity with electron rich groups, and contrary to that, blue regions represent electron deficient regions and can lead to an increase in the activity of molecules by similar substitutions.

A careful analysis of the contours of the  $\alpha$ ,  $\gamma$ , and  $\delta$  models (Fig. 4) revealed that most of the contours are found in the variable side chain while few are found in the acidic part. It was also revealed that electrostatic contributions are relatively more in

$\alpha$  model and the steric fields play an important role in the  $\gamma$  model. But the contours of the  $\delta$  model were not found to reveal much relevant information. The contour maps of  $\alpha$  model clearly showed that steric bulk and electronegative groups at the variable side chain of the most active molecule **1n** may improve biological activity at PPAR $\alpha$ .

The contours of dual model reveal that electrostatic contributions which are predominant in  $\alpha$  model also exhibit similar significance in the dual model. Steric contours reflect the addition of steric fields from  $\alpha$  and  $\gamma$  models. Electrostatic features furnished by electrostatic contours of dual model are responsible for  $\alpha$  activity and steric features furnished by steric contours of dual model enhance activity at both  $\alpha$  and  $\gamma$  receptors. High affinity dual activators for PPAR $\alpha$  and PPAR $\gamma$  receptors show good field fit in contour maps of all three models. For example though a slight destabilizing interaction is observed in electrostatic contours of dual  $\alpha/\gamma$  and  $\alpha$  model, **1k** shows comfortable fit into the contour maps of all three CoMFA models. On the other hand, **2g** shows unfavorable electrostatic overlaps and unfavorable steric overlaps in contours of  $\gamma$  model. **2g** also does not fit well in the contours of  $\alpha$  model as well as dual  $\alpha/\gamma$  model. **1c** and **2a** which do not fit well in dual  $\alpha/\gamma$  model also show reasonably poor field fit in  $\alpha$  model and  $\gamma$  model. These examples clearly show that a comparative analysis is useful in validating the dual model because those molecules which find proper field fit in dual model also find proper field fit in both the  $\alpha$  and  $\gamma$  models.

The contour map analysis of  $\alpha$ -CoMFA model indicates that the *meta* as well as *para* positions of the phenyl substituents on the oxadiazole ring are covered by green and red contours. This indicates that sterically bulky substituents along with electronegative substituents favour PPAR $\alpha$  activity. For example **1n** with two CF<sub>3</sub> groups at *meta* position as well as **1k** with isopropyl group are more active because in these systems the bulky and electronegative groups are entering into the red and green contours. On the other hand, the contour maps of PPAR $\gamma$  indicate that bulky but less electronegative substituents are more favorable at the *meta* and *para* positions of the phenyl ring. The contour maps of  $\alpha/\gamma$  dual model do possess the additive character of contour maps  $\alpha$  and  $\gamma$  individual CoMFA models. The steric contour map of the dual model supports bulky groups for both  $\alpha$  and  $\gamma$  activity. The electrostatic contour plot of dual model is covered by blue region on one side and the red region on the other side of the phenyl ring. This indicates that for improved dual activity one of the *meta* substituent should have electronegative group whereas the other should be less electronegative while both can be sterically bulky. Thus modulation of PPAR agents with electronegative bulky group at one *meta* position and electropositive bulky group at the other *meta* position should favour the improvement of dual activity. For example the newly designed molecule **2i** (Fig. 5) shows good predicted  $pEC_{50}$  ( $M$ ) according to  $\alpha$ -CoMFA model (7.8234),  $\gamma$ -CoMFA model (7.2083) and better predicted  $pEC_{50}$  ( $M$ ) according to  $\alpha/\gamma$  dual model (16.3312). This is further verified by FlexX based molecular docking of this molecule in the active sites of PPAR $\alpha$  and PPAR $\gamma$ .

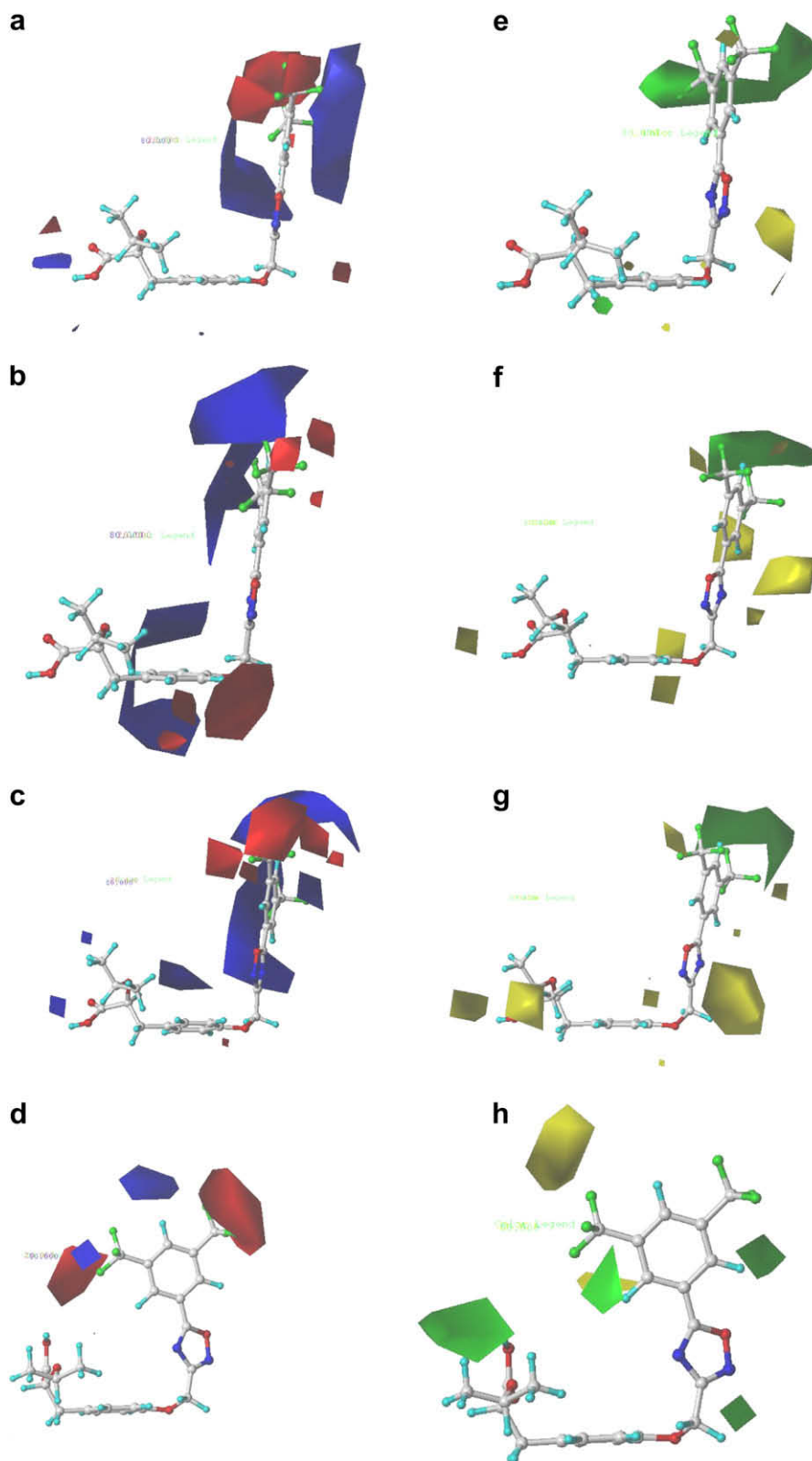
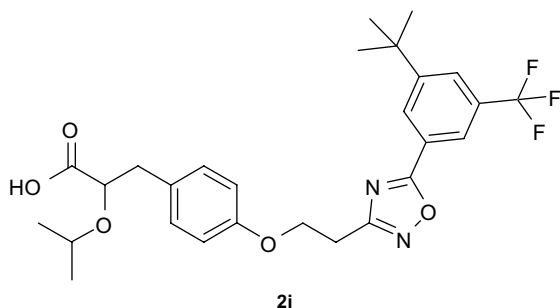


Fig. 4. (a–d): Electrostatic contour maps for  $\alpha$ ,  $\gamma$ ,  $\alpha/\gamma$  and  $\delta$ , respectively; (e–h): steric contour maps for  $\alpha$ ,  $\gamma$ ,  $\alpha/\gamma$  and  $\delta$ , respectively.

#### 4. Conclusions

Comparative Molecular Field Analysis (CoMFA) methodology was adopted to identify the correlation between the reported

PPAR $\alpha$ , PPAR $\gamma$  and PPAR $\delta$  activators of a single series of compounds with their biological activities. Very robust CoMFA models could be obtained for PPAR $\alpha$  and PPAR $\gamma$ . On the other hand, the CoMFA model for PPAR $\delta$  was found to be statistically

Fig. 5. Structure of **2i**.

weak. Dual CoMFA model for PPAR $\alpha$  and PPAR $\gamma$  was found to be very robust and more informative than individual CoMFA models. This confirmed that additivity concept is worth pursuing further. However, the development of dual CoMFA models involving PPAR $\delta$  data did not succeed. This follows from the poor performance of the PPAR $\delta$  CoMFA model. This may be originating from the partial agonistic character of the ligands against PPAR $\delta$ . This work helps us to identify an additional limitation of CoMFA model i.e. when the data associated with any target is poorly correlated, this data may not be useful for generating dual activators. Though this limitation can be generally expected, explicit evidence for this was not previously reported. The poor correlation of the PPAR $\delta$  data also leads to the failure in developing PPAR $\alpha/\gamma/\delta$  multiple model. Thus the question whether or not the additivity concept can be extended to multiple activators could not yet be ascertained.

### Acknowledgements

The authors acknowledge the financial support from Department of Science and Technology and Council of Scientific and Industrial Research, New Delhi for carrying out this work.

### References

- [1] R. Morphy, Z. Rankovic, *J. Med. Chem.* 48 (2005) 6523–6543.
- [2] R. Morphy, C. Kay, Z. Rankovic, *Drug Discov. Today* 9 (2004) 641–651.
- [3] A. Gangjee, J. Yu, J.J. McGuire, V. Cody, N. Galitsky, R.L. Kisliuk, S.F. Queener, *J. Med. Chem.* 43 (2000) 3837–3851.
- [4] A. Gangjee, J. Yu, R.L. Kisliuk, W.H. Haile, G. Sobrero, J.J. McGuire, *J. Med. Chem.* 46 (2003) 591–600.
- [5] S.H. Lee, M.J. Son, H.K. Ju, C.X. Lin, T.C. Moon, H.-G. Choi, J.K. Son, H.W. Chang, *Biol. Pharm. Bull.* 27 (2004) 786–788.
- [6] C. Charlier, C. Michaux, *Eur. J. Med. Chem.* 38 (2003) 645–659.
- [7] G. Gaetano, M.B. Donati, C. Cerletti, *Trends Pharmacol. Sci.* 24 (2003) 245–252.
- [8] R. Shan, C. Velazquez, E.E. Knaus, *J. Med. Chem.* 47 (2004) 254–261.
- [9] S. Khanna, M.E. Sobhia, P.V. Bharatam, *J. Med. Chem.* 48 (2005) 3015–3025.
- [10] I.I. Baskin, I.G. Tikhonova, V.A. Palyuin, N.S. Zefirov, *J. Med. Chem.* 46 (2003) 4063–4069.
- [11] B.R. Henke, *J. Med. Chem.* 47 (2004) 4118–4127.
- [12] B. Staels, J. Auwerx, *Curr. Pharm. Des.* 3 (1997) 1–14.
- [13] B.M. Spiegelman, *Diabetes* 47 (1998) 507–514.
- [14] R. Kumar, U. Ramachandran, S. Khanna, P.V. Bharatam, S. Raichur, R. Chakraborti, *Bioorg. Med. Chem.* 15 (2007) 1547–1555.
- [15] P.V. Bharatam, S. Sundriyal, *J. Nanosci. Nanotech.* 6 (2006) 3277–3282.
- [16] S. Khanna, R. Behal, P.V. Bharatam, in: S.P. Gupta (Ed.), *Topics in Heterocyclic Chemistry*, vol. 3, Springer-Verlag, Heidelberg, 2006, pp. 149–180.
- [17] P.V. Bharatam, S. Khanna, *Indian J. Chem.* 45A (2006) 188–193.
- [18] P.V. Bharatam, S. Khanna, *J. Phys. Chem. A* 108 (2004) 3784–3788.
- [19] U. Ramachandran, R. Kumar, A. Mital, *Mini Rev. Med. Chem.* 6 (2006) 563–573.
- [20] M. Ahmed, S. Khanna, P.V. Bharatam, *Indian J. Chem.* 44B (2005) 600–606.
- [21] R.W. Oliver, J.L. Shenk, M.R. Snaith, C.S. Russell, K.D. Plunket, N.L. Bodkin, M.C. Lewis, A.W. Deborah, M.L. Sznajdman, M.H. Lambert, H.E. Xu, D.D. Sternbach, S.A. Kliewer, B.C. Hansen, T.M. Willson, *Proc. Nat. Acad. Sci. U.S.A.* 98 (2001) 5306–5311.
- [22] K.G. Liu, J.S. Smith, A.H. Ayscue, B.R. Henke, M.H. Lambert, L.M. Leesnitzer, K.D. Plunket, T.M. Willson, D.D. Sternbach, *Bioorg. Med. Chem. Lett.* 11 (2001) 2385–2388.
- [23] SYBYL6.9, Tripos Inc., 1699 S. Hanley Rd., St. Louis, MO 63144, USA, 2002.
- [24] H.E. Xu, M.H. Lambert, V.G. Montana, K.D. Plunket, L.B. Moore, J.L. Collins, J.A. Oplinger, S.A. Kliewer, R.T. Gampe, D.D. McKee, J.T. Moore, T.M. Willson, *Proc. Nat. Acad. Sci. U.S.A.* 98 (2001) 13919–13924.
- [25] H.E. Xu, M.H. Lambert, V.G. Montana, D.G. Parks, S.G. Blanchard, P.J. Brown, D.D. Sternbach, J.M. Lehmann, B.G. Wisely, T.M. Willson, S.A. Kliewer, M.V. Millburn, *Mol. Cell* 3 (1999) 397–403.
- [26] R.T. Nolte, B.G. Wisley, S. Westin, J.E. Cobb, M.H. Lambert, R.K. Urokawa, M. Rosenfeld, *Nature* 395 (1998) 137–143.
- [27] R.S. Mulliken, *J. Chem. Phys.* 23 (1955) 1833–1840.
- [28] R.D. Cramer, D.E. Patterson, J.D. Bunce, *J. Am. Chem. Soc.* 110 (1988) 5959–5967.